West Chester University

Digital Commons @ West Chester University

Spring 2020

Microbial Energy Storage and Antimicrobial Effects of Metal Nanoparticles

Octavia Allen
oa920253@wcupa.edu

Microbial Energy Storage and Antimicrobial Effects of Metal Nanoparticles

A Thesis

Presented to the Faculty of the

Department of Biology

West Chester University

West Chester, Pennsylvania

In Partial Fulfillment of the Requirements for the

Degree of

Master of Science

By

Octavia A. Allen

May 2020

Acknowledgements

There are a number of individuals I would like to acknowledge and thank for their role in helping me complete my thesis work. I would like to thank the faculty and students of West Chester University's Biology Department for their encouraging words while I was working on this project for the past 2 years. Also, to Enrique Mentado and Jim Wheeler, thank you for assisting me with learning new lab techniques and how to utilize certain lab instruments. Jim, thank you so much for your time and lending your strong chemistry background knowledge for the benefit of this project. To Samantha Shumlas, thank you for allowing me to use the Center for Microanalysis and Imaging Research and Training (CMIRT) Facility and helping with obtaining results from using X-ray Diffraction, Energy-Dispersive X-ray Spectroscopy, and Scanning Electron Microscopy.

To my committee members, Dr. Pisciotta, Dr. Mbuy, and Dr. Pagán, thank you for all your help, advice, and patience. All of you have been so helpful in not only the completion of this project, but also great mentors for anything I had questions about. Thank you for teaching me so much about the field of microbiology, bioenergy, and being there for me every single step of the way Dr. Pisciotta. I truly appreciate it; you are an awesome advisor! Lastly, but certainly not least, I would like to thank God. It was God who blessed me with the strength, determination, ambition, patience, and focus to complete this thesis project. I literally would not have been able to successfully complete this work without Him.

Abstract

Microbial Energy Storage and

Antimicrobial Effects of Metal Nanoparticles

By Octavia A. Allen

Chairperson: John Pisciotta, PhD

With the use of Microbial Electrolysis Cells (MECs) and anaerobic digester (AD) designs, wastewater treatment could be more effectively processed. Inoculation of anaerobic microorganisms, methanogens specifically, can help convert organic matter in wastewater metabolizing it to produce CH_4. Most MECs are stationary and are not actively mixed to promote expedited CH_4 production. The objective of this work was to design Wind-Actuated Vibrating Electrochemical (WAVE) digesters and utilize electrical current to increase CH_4 production rates generated by anaerobic microorganisms in MECs, optimizing efficiency of wastewater treatment. It was hypothesized WAVE mixed digesters will enhance conversion of wastewater into biogas compared with conventional AD designs, and faster startup of biogas production will occur in WAVE actuated digesters vs controls. Also, higher voltage of 900 mV will result in greater biogas production compared to 700 mV or conventional AD (i.e. disconnected).

Current was applied at 700 mV and 900 mV to specified reactors in coordination with vertical and horizontal WAVE digester designs. Concluding experimentation, there was no significant difference between voltage or WAVE digester design on CH_4 production concluding the 8-week study. Compared to the stationary, traditional anaerobic digester, none of the 700 mV applied MECs, despite WAVE digester design, had a significantly higher CH_4 accumulation after 8 weeks. Compared to the stationary, traditional anaerobic digester, none of the 900 mV applied MECs, despite WAVE digester design, had a significantly higher CH_4 accumulation after 8

weeks Compared to traditional anaerobic digesters, CH_4 recovery while treating wastewater is optimized in digesters with an applied voltage.

Table of Contents

List of Tables

List of Figures

Introduction

Wastewater Treatment

Wastewater treatment is a significant routine practice in society, as it forestalls an over-burdening of pathogenic contaminants and chemical substances from being discharged and released into natural waterways. Wastewater can accumulate from household and societal sewage waste, and storm water runoff, which collects pollutants from roads, rooftops, and agriculture fields (Quinn, 2019). Modern wastewater treatment plants involve multiple stages including but not limited to: bulk filtration, primary settling, aeration and nitrification, secondary settling, clarification and denitrification and chemical disinfection prior to release of effluent downstream (Quinn, 2019).

Wastewater treatment is an energy intensive process that accounts for roughly 2% of the nation's electrical energy use (*Center for Sustainable Systems*). Around 63% of this energy is derived from fossil fuels like coal or natural gas generated electricity (*U.S. energy facts—Data and statistics—U.S. Energy Information Administration (EIA)*, n.d.). The use of fossil fuels contributes to the release of greenhouse gases, which commonly happens when an energy-intensive, electrically driven process such as aerobic wastewater treatment technologies are operated around the clock.

Directly vented gas from aerobic wastewater treatment operations are composed of approximately 50% carbon dioxide (CO_2), 50% methane (the primary component of natural gas), and a very small amount of non-methane organic compounds (US EPA, 2016). Although both methane and CO_2 are greenhouse gases and play roles in the continuation of global warming, methane is 28 to 36 times more effective than CO_2 at trapping heat in the atmosphere over a 100-

year period (US EPA, 2016). In 2016, the third-largest source of human-related methane emissions in the U.S. came from municipal solid waste landfills, accounting for about 14.1% of these emissions (US EPA, 2016).

Recovery of biogas energy from landfill waste as well as wastewater is possible; however, more methane can be collected and prevented from migrating into the atmosphere where it contributes to local smog and global climate change. Covered anaerobic digesters can collect the generated methane gas (CH_4) and be designed for increased efficiency. As methane emits freely into the atmosphere from landfills and wastewater plants, much opportunity is lost to capture and use a significant renewable energy resource that could otherwise help offset fossil fuel-generated power used to power the facilities.

Anaerobic Digestion

Anaerobic digestion is the process of treating organic waste as it is broken down using diverse, naturally present microorganisms in the absence of oxygen. Instead of releasing methane gases into the air, a more productive use would be to use it as an energy source (*Facts About Anaerobic Digesters*, 2018). Renewable biogas energy sources are increasingly being used as alternatives to traditional fossil fuels. In 2018, about 11% of the United States' total energy consumption came from renewable energy sources, and 17% of the nation's electricity generation was from renewable energy (*U.S. Energy Information Administration (EIA)*). With the use of anaerobic digestion, anaerobic microorganisms that are housed in these anaerobic digestors grow and facilitate the breakdown of organic compounds present in the wastewater.

The synergetic interactions of microorganisms that decompose organic polymers to smaller molecules are what determine the success of anaerobic digestion processes (Alcántara-

Hernández et al., 2017). There are three main phases of anaerobic digestion for biogas which are carried out by different groups of prokaryotes. The first phase is hydrolysis, which is the rate limiting step, and fermentation. During this phase, polymeric components of organic waste including proteins, lipids and carbohydrate are enzymatically broken down into smaller fermentable dimmers and monomers. Acidogens are the primary fermentative microbes that decompose complex organic matter to acetic acid and other acids (Wall et al., 2008). These acidogens also break down organic matter to higher volatile fatty acids (mainly propionate and butyrate), H_2, and CO_2 (Wall et al., 2008). The higher volatile fatty acids are decomposed by H_2 - producing acetogenic groups to form acetate, H_2, and CO_2 (Wall et al., 2008).

Acetogenesis, or phase two of biogas formation, is the fermentation of those products consumed, namely CO_2 and H_2 by acetate generating acetogens. These chemolithotrophic acetogens, mainly of the genera *Clostridium* and *Sporomusa*, utilize the H_2 as their energy source to fix the CO_2 and then release acetate generated via the reverse acetyl Co-A pathway (Wall et al., 2008), also called the Wood Ljungdahl pathway. The third phase is methanogenesis and if facilitated by two main groups of methanogens. Methanogens are members of the *Archaea* domain and are of the *Euryarchaeota* kingdom. Methanogens are strict anaerobic microorganisms that are responsible for carrying out methanogenesis. The end product of their metabolic process is biogas, which is a methane-rich gas.

The metabolic products of the fermentative and acetogenic groups are converted to CH_4 by methanogens via two major pathways: hydrogenotrophic and acetoclastic routes. During hydrogenotrophic methanogenesis, H_2 is oxidized to $2H^+$, and CO_2 is reduced to CH_4 ($CO_2 + 4H_2$ Methanogenesis $\rightarrow CH_4 + 2H_2O$). Acetoclastic methanogens catabolize acetate formed chiefly by acetogens to form CH_4 and CO_2. They are found in habitats where hydrogenotrophic

methanogens reduce H_2 levels low enough to create the conditions needed for high levels of acetate formation. Conversion of the methyl group of acetate by acetoclastic microbes accounts for at least two-thirds of the CH_4 produced in nature (Wall et al., 2008). The methanogenic hydrogenotrophic group produces about one-third of the CH_4 by reducing CO_2 with electrons supplied from the oxidation of H_2 (Wall et al., 2008). Methanogens are dependent on those first two phases of anaerobic digestion to supply the necessary substrates for their growth. Despite its relatively low energy yield, methanogenesis is a dominant pathway for organic matter decomposition in terminal electron acceptor limited environments.

Bioelectrochemical Systems (BESs)

Traditional anaerobic digestion has certain advantages, like biofuel production, but there is room for improvement. Because product compounds are not fully oxidized, energy will be available in biogas with the use of anaerobic digestion. The greenhouse gasses which were once released, will instead be retained in the reactor and used as substrate to be catabolized by the anaerobic microorganisms. This reduces the amount of available CO_2 in the atmosphere and increases the amount of CH_4 produced. Over the past few years, bioelectrochemical systems (BESs) have become more popular for their contribution as an emerging sustainable technology for both electricity production and wastewater treatment or accelerated biogas formation (Bajracharya et al., 2016). BESs are unique systems that use microbes (and/or their products) for converting chemical energy into electrical energy, or vice-versa, to provide useful renewable energy (Bajracharya et al., 2016). BESs use whole-cells, usually bacteria, as biocatalysts to drive oxidation and reduction reactions at an electrode (anode) and counter electrode (cathode), respectively. The anaerobic digestion of organic waste offers major environmental and economic

benefits including: production of biogas from non-fossil sources, retention of gases with greenhouse effect, reduced landfilling requirements, reduction of pathogenic microorganisms, reduction of odors and flies, and the coproduction of a digestate from sludge with high fertilization capacity (Holm-Nielsen et al., 2009).

Better understanding of the electron transfer mechanisms could give insight into methods to steer the processes towards higher rates. The fermentation of wastes, such as plant waste, may also produce acetic acid that can be catabolized by exoelectrogens and/or methanogens. The exoelectrogenic microorganisms (ex. *Geobacter sulfurreducens, Geobacter metallireducens*) catabolize an organic substrate (ex: acetate) and release electrons, protons, and CO_2 at the anode. This causes substrate oxidation reaction on the anode with anode reduction. This metabolic process continues as exoelectrogenic microorganisms deposit electrons onto the anode and a negative charge builds. Once the anode is saturated with electrons, an electrical current transits through an external circuit to the cathode. However, the cathode reduction reaction is not spontaneous in a microbial electrolysis cell (MEC), and an applied voltage is needed. The current from the deposited electrons in conjunction with an outside power source, such as a solar panel, stimulates reduction at the cathode. Protons released by the exoelectrogenic bacteria diffuse through an ion exchange membrane to the cathode in response to its imbalanced electrochemical gradient. Electrons join the protons at the cathode. Electrotrophic microbes on the cathode accept electrons, reducing protons to form hydrogen gas. This H_2 can facilitate the growth and metabolism of hydrogenotrophic methanogens.

In methane producing BESs, microorganisms grow on a cathode and catalyze the conversion of CO_2 and electricity into methane via a process called direct electromethanogenesis (Xu et al., 2019). Theoretically, methane can be produced bioelectrochemically from CO_2 via

either direct electron transfer or indirectly via hydrogen, acetate or formate (Eerten-Jansen et al., 2012). In the past decade, MECs have been investigated for their potential integration into current wastewater treatment technologies to generate methane at a faster rate and further decontaminate organic material present in wastewater.

Microbial Electrolysis Cells (MECs)

Certain methanogens are electrotrophic *Archaea* that occupy the cathode. They reduce the CO_2 and store input electrical energy as chemical fuel bonds, biofuel. Harvesting methane at the cathode of MECs could accelerate the rate of anaerobic digestion. Microbial electrolysis cells (MECs) operate under relatively mild conditions and do not use expensive precious metals as catalysts. The recently discovered MEC has greatly expanded the horizon for BESs. This could be a clean alternative avenue of collecting greenhouse gases, methane specifically, rather than using fossil fuel combustion reactions. It can reduce the amount of energy needed to produce biofuels by using the natural redox potentials of the microorganisms that occupy the anionic and cationic chambers of the MECs (Eerten-Jansen et al., 2012).

MECs can be produced by modifying a microbial fuel cell (MFC) in two ways: adding a very small amount of voltage at the anode; and not allowing any oxygen at the cathode (Choi et al., 2017). A study was done where MECs at various cell voltages (0.5, 0.7, 1.0 and 1.5 V) were operated in anaerobic fermentation (Choi et al., 2017). These voltages were applied the MECs to test whether the rate of methane production would be affected. The optimization of external energy (current and voltage) plays a key role in product formation and CH_4 generation and chemical oxygen demand (COD) degradation (Zhao et al., 2016).

Normally electrolysis of water occurs approximately at 1.0 V. A downside of using traditional anaerobic digestion is that it takes weeks for the start-up process to happen, because these anaerobic microbes grow at such a slow pace. Even though the microbial community composition of anaerobic digestion has been long studied via culture-dependent and independent molecular methods (Alcántara-Hernández et al., 2017), most of these studies characterize the bacterial component in well-established reactors. It is still not clearly understood how microbes respond to substrate variations during the reactor start-up and working processes (Alcántara-Hernández et al., 2017).

The growth of exoelectrogenic bacteria, especially *Geobacter* species, is boosted in MEC anaerobic digestion, which results in the accelerated decomposition of substrates (Xu et al., 2019). Metals used to investigate anaerobic digestion with different types of conductive materials have been studied as well. The decomposition of complex organics in the presence of conductive Fe(III)/Fe(III)-Fe(II) oxides was accompanied by the significant production of hydrogen, which resulted in the increase of hydrogen partial pressure as well as the enrichment of hydrogen-utilizing methanogens (Zhao et al., 2017).

Modifications of BESs for Methane Production Enhancement

From the data and background information observed, an experiment testing neglected aspects of MECs, and anaerobic digestion could be conducted to further advance this groundbreaking field. MECs have previously been studied and various voltages have been tested in order to speed the rate of methane production (Choi et al., 2017; Xu et al., 2019). In order to promote the rate of methane production with anaerobic digestion using MECs alternative variable were tested in this study. Anaerobic digestion is an ever-growing area of interest with

the new advances of BESs. These BESs have the potential to change an entire industry in wastewater treatment, and it has the opportunity to exert a positive impact on the combustion and release of greenhouse gases around the world. In this study, the hypotheses tested were that WAVE mixed digesters will enhance conversion of wastewater into biogas compared with conventional AD digesters. Also, faster startup of biogas production will occur in WAVE actuated digesters vs controls, and a higher voltage of 900 mV will result in greater biogas production compared to 700 mV or AD, disconnected.

Materials and Methods

Microbial Energy Storage

WAVE Digester Design

Fundamental reactors required for each WAVE digester were built at a 100 mL lab scale. For each reactor, 1 cm x 4 cm stainless steel mesh cathodes were inserted into each 100 mL glass vial and connected via 8 cm titanium wires pressed through a rubber stopper. A total of 18, 100 mL serum vials were each filled with 85 mL of pH 7.0, 50 mM phosphate buffer containing 0.5 g/L acetate. For the anode counter electrode, a graphite plate measuring 1 cm x 4 cm x 0.3 cm was crafted and connected to titanium wire (see Figure 2A). Each reactor was sealed with a rubber stopper and crimped capped. Three control vials without anodes or cathodes were used to simulate conventional anaerobic digesters. All vials were then autoclaved, and appropriate vials were inoculated with 3 mL of inoculum form an established digester. One vial served as the sterile control and was not inoculated.

Construction of WAVE digesters: The WAVE digesters were assembled as vertical and horizontal rotors using 1 central aluminum tube (arrow), 2 fidget spinners, 6 bolts with screws, 1 skateboard wheel, 3 small screws (head is 1.2 mm), 39 zip ties, 1 rotating electrical contactor, and 6 41 x .2 cm aluminum sticks each (see Figure 1A). Vertically and horizontally mixed rotors were assembled to determine optimal device configuration. Two sets of triplicate reactor vials were attached to each rotor. Each reactor vial was then assigned a potentiostat channel and voltage (see Figure 3A). There were 3 traditional anaerobic digesters (AD) that were disconnected. There were 3 control stationary MECs set to 700 mV. There were 6 vials per rotor. So, 3 of the 6 vials of each rotor was set to 700 mV, while the other 3 were set to 900 mV.

Inoculation: The reactors were retrieved from the autoclave and the needles were removed from them immediately. Necessary precaution was taken to prevent the threat of too much O_2 exposure to the microorganisms. A nitrogen insulated bag was injected into each vial to make sure when the pressure inside the MECs matched that of the atmosphere, the MEC will absorb nitrogen instead of O_2. Once the reactors were cooled at room temperature, they were inoculated with 3 mL of a mixed culture of anaerobic microorganisms from an established digester used in a prior experiment.

Quantification of Electrogenic Activity

Gas Chromatography: The gas chromatograph (GC) used to identify and quantify biogases produced from the strict anaerobic microorganisms was the SRI 8610C Gas Chromatograph Multiple Gas #3 GC configuration. It is a versatile way of analyzing many different kinds of gas samples. The GC has two Multiple Gas #3 (MG#3) configurations implemented in a single GC chassis so there are two gas sampling valves and 2 columns as well as 2 detectors: TCD or FID. Nitrogen was used as the carrier gas. After injecting the calibration standard gas (CO_2, H_2, CO, CH_4, O_2), standard curves were calculated in order to properly calibrate the GC for the identification of each gas tested.

Five of the MECs (control, #1, #5, #9, #12) were tested by using the GC, confirming there was no O_2 present. O_2 inhibits the growth of strict anaerobes, and there was no O_2 detected in any of the 200 μL headspace gas samples. Gas samples were taken weekly and analyzed via GC after the rotors were assembled and vials inoculated. The area under the curve was analyzed and recorded. The two main gasses of interest were methane (CH_4) and carbon dioxide (CO_2).

Chronoamperometry: A potentiostat is a device that controls the potential between a pair of electrodes while measuring the resulting current flow. For maintaining constant electrical current to each reactor's electrodes, a Biology MPG-2 Potentiostat was used. The potentiostat was set to 700 mV and 900 mV for the duration of the WAVE digester experiment.

Microbial Community Analysis

DNA Extraction: The PowerBiofilm DNA Isolation Kit was used to isolate the DNA from the mixed culture sample and procedure A (PowerLyzer 24 Homogenizer) was followed to carry out the DNA isolation. First, 0.05 to 0.20 g of biofilm material was weighed out and placed into a 2 ml Collection Tube. The biofilm material was then centrifuged at 13,000 x g for 1 minute. The supernatant was removed using a pipette tip. Then, the biofilm material was resuspended in 350 µL of Solution BF1 and transferred to the PowerBiofilm Bead Tube. 100 µL of Solution BF2 was added to the tube and vortexed briefly to mix. Then, the PowerBiofilm Bead Tube was incubated at 65°C for 5 minutes.

The sample was mixed with bead beaters following procedure A, PowerLyzer 24 Homogenizer. To maintain organization, it was made sure to properly identify each PowerBiofilm Bead Tube on both the cap and on the side. Placed Bead Tubes into the Tube Holder of the PowerLyzer 24. The Bead Tubes were balanced (evenly spaced) on the Tube Holder and homogenized for 1 cycle at speed 3200 RPM for 30 seconds. The tube was centrifuged at 13,000 x g for 1 minute. Then, the supernatant was transferred to a new 2 ml Collection Tube.

100 µl of Solution BF3 was added and vortexed briefly to mix, then incubated at 4°C for 5 minutes. Centrifuged the tube at 13,000 x g for 1 minute at room temperature. Transferred the entire volume of supernatant to a clean 2 mL Collection Tube, avoiding the pellet. Added 900 µL of Solution BF4 and vortexed briefly to mix. Loaded 650 µL of supernatant onto a Spin Filter and centrifuged at 13,000 x g for 1 minute. Discarded the flow through and repeated until all the supernatant had been loaded onto the Spin Filter. Placed the Spin Filter basket into a clean 2 mL Collection Tube, then inverted Solution BF5 8 times to mix before use. Added 650 µL of Solution BF5 and centrifuged at 13,000 x g for 1 minute at room temperature. Discarded the flow through and added 650 µL of Solution BF6 and centrifuged at 13,000 x g for 1 minute at room temperature. Then, discarded the flow through and centrifuged again at 13,000 x g for 2 minutes to remove residual wash. Afterward, placed the Spin Filter basket into a clean 2 mL Collection Tube and added 100 µL of Solution BF7 to the center of the white filter membrane. Centrifuged at 13,000 x g for 1 minute, then discarded the Spin Filter basket. The DNA was then ready for any downstream application.

DNA Quantification: The quantification was carried out using a NanoDrop Spectrophotometer. The NanoDrop is a full spectrum UV-Vis spectrophotometer used to quantify and assess purity of DNA, RNA, and protein. This microvolume spectrophotometer has the unique ability to measure sample volumes as small as 0.5 µL.

16S rDNA PCR Amplification: 16S rDNA is a section of prokaryotic DNA that codes for a gene found within all bacteria. Within bacterial cells the rRNA transcribed from the 16S rDNA gene forms the small subunit of the ribosome. The 16S rDNA gene is one of the most conserved genes of all. This means that it has undergone very little change throughout time, or it varies very

little from cell to cell. Even prokaryotes that are distantly related, or that evolved a long time ago, have 16S rDNA sequences that are similar.

Scientists use this gene, as well as other ribosomal genes, to measure taxonomy, phylogeny and the rate of evolutionary divergence. Within microorganisms, the study of the 16S rDNA gene has been used to look at how single celled organisms are related. In particular, any variations in the gene are noted and compared to other bacterial cells. Examining these differences allows researchers to form evolutionary links between different organisms.

After isolation of the DNA, it was then amplified using polymerase chain reaction (PCR). The forward primer, 338 1:10, and backward primer, 907 1:10, in addition to Taq polymerase and nuclease-free water which were added to the reaction mixture before running the DNA samples through the PCR. The reaction mixture was made of 6.25 µL of 338 1:10 primer, 6.25 µL 907 1:10 primer, 312.5 µL Taq polymerase, and 275 µL DNA nuclease free H_2O. After the reaction mixture was made, 24 µL of the reaction mixture was distributed to 24 PCR tubes and 1 µL of each DNA sample was added to its respective PCR tube. Once all the necessary solutions were added to each PCR tube, the mixture was inverted 8 times and ready to be put into the thermocycler. The PCR settings were first set to have optimal amplification. The denaturation temperature was 95 °C to separate the double strands, the annealing was 53 °C so the 338 1:10 and 907 1:10 primers would anneal to the DNA, and the extension stage was set to 72 °C allowing the Taq polymerase to extend the template sequence and copy the DNA. This three-stage process was set to repeat 35 times, yielding numerous copies of the DNA.

Denaturing Gradient Gel Electrophoresis (DGGE): DGGE was used to separate the PCR generated DNA products. PCR products from a given reaction are of similar size (bp), conventional separation by agarose gel electrophoresis results only in a single DNA band that is

13

largely non-descriptive. DGGE can overcome this limitation by separating PCR products based on sequence G:C and A:T differences that results in differential denaturing characteristics of the DNA. The gel assembly was built by using gel clamps, a well comb and spacers between two glass plates. The DGGE gel composition gradient was comprised of 120 µL of 10% Ammonium Persulfate (APS) and 6 µL of Tetramethylenediamine (TEMED) added to both the low denaturant concentration solution, and a high denaturant concentration solution. The solutions in both chambers of the gradient maker were released into the assembled glass gel sandwich, then allowed to settle out with the well comb inserted. Once the polyacrylamide gel polymerized, the complete gel apparatus was assembled, and 25 ng of DNA from each selected reactor was loaded into its designated well. The DGGE was set to 90 V and was ran for 24 hours. When the electrophoresis was complete, the gel was stained then analyzed using a UV transilluminator.

Nanopore DNA Sequencing: The MinION streams data in real time so that analysis can be performed during the experiment and workflows are versatile. The Nanopore MinION works by passing a current across DNA permeable electrically-resistant membranes into which protein nanopores are embedded. As DNA moves through the nanopore it causes a base-specific disruption in the current. This electric disruption can be used to analyze the sequence of bases. The MinION Oxford Nanopore sequencing kit process began after downloading the Nanopore program to the computer and the Nanopore DNA library processing was completed. The DNA was added to the flow cell of the MinION. The flow cell contains a sensor that detects the characteristic nanopore signal as the molecule is analyzed. After the flow cell had been filled with the DNA sample, the MinION was ran and sequencing began. When the sequencing was completed, Geneious, a sequencing analysis program, was used to group similar sequences together. By using the align tool in Geneious to group similar sequences together, the familial

tree was exported from the program into the National Center for Biotechnology Information (NCBI) Basic Local Alignment Search Tool (BLAST) search. The BLAST search compares nucleotide or protein sequences to sequence databases and calculates the statistical significance of matches. BLAST can be used to identify unknown or new sequences, infer functional and evolutionary relationships between sequences, and identify members of gene families. After the blasted sequences were completed, the identified microbial species were observed, and the lineages were phylogenetically analyzed.

Antimicrobial Effects of Metal Nanoparticles

Anti-Microbial Metals

To test the effect of anti-microbial metals, Cu used as the focal cathode acting as an unchanging variable. The comparison of metals were the pair of Fe anode and Cu cathode versus a Zn anode and Cu cathode. T4 bacteriophage was used as the virus of interest in this pivotal portion of the experiment. Because we used the T4 bacteriophage, *E. coli* b-strain (from Carolina Biological Supply Company) was the desired host cell for optimal plaque assay analysis.

Waterborne Viruses and Indicator Species

Our species of interest was *E. coli* b-strain. An EMB agar dish was used to isolate the microbe colonies and validate that they are indeed *E. coli*. An *E. coli* b-strain colony was recovered from the EMB agar and put into a tube of TSB broth. The agar plate was then incubated at 37°C. Afterwards, we prepared 100mL of LB top agar. Then, 5 mL of the LB top agar was distributed into glass tubes. After the LB top agar was distributed, the tubes and agar

were autoclaved and stored in a warming oven. An isolated colony of our targeted *E. coli* b-strain was collected, then used the Beckman Coulter DU650 Spectrophotometer to analyze the optical density of the *E. coli* b-strain from the TSB to determine approximate level concentration, measured in cfu/mL.

   Plaque Assay Procedure: The autoclaved stopper was inserted with the respective metals into each vial. Afterward, I injected T4 bacteriophage into the 0 V vial and made sure to shake well. Connected the vial to the power supply (Cu, cathode; Fe, anode) at 0 V for 10 minutes and observed the gas volume that was displaced by inserting a syringe. Withdrew 0.5 mL of the voltaged solution and placed it in the labeled undiluted test tube. Added 450 µL of sterilized water to the remaining plastic test tubes. Pipetted 50 µL from the undiluted tube into the next one to begin the serial dilution, mixing it by gently pipetting the mixture up and down.

   Repeated the previous steps for voltages 5, 10, and 15 as well. Once the 15 V dilution series was complete, 500 µL of each diluted sample (undiluted, -1, -2, etc.) was injected into their respective top agar tubes. Added the optimal number of µL of the log phase *E. coli* B into the injected top agar tubes. Poured the top agar mixture onto its respective labeled bottom agar plate and repeated these steps for all voltages (0, 5, 10, and 15). Incubated the poured plates at 37°C. The number of plaques were observed and analyzed the next day.

Effects of Various Metals on Gas Production Rates

   To test the optimization of gas production rates by using different metals, 100 mM NaCl solution with distilled H_2O was prepared. Then, 100 mL were distributed to 12 vials and capped with a rubber stopper. Fe, Zn, Al and Ti anodes were cut to measure 7.5 cm, and Cu cathodes were cut to be 5 cm in length. The filled vials and electrodes were autoclaved for sterility. Once

sterile and cooled to room temperature, a Cu cathode and Fe anode was inserted into each vial through the rubber stopper. The assembled vials were connected to a power supply and set to 0 V, 5 V, 10 V, and 15 V for 10 minutes each. Each voltage was ran 3 times with 3 assembled vials to perform triplicates. Gas production was measured by inserting a syringe into the vial and observing the plunger displacement volume. Once completed, the vials were emptied, washed, more 100 mM NaCl solution was prepared, and the process was repeated with a different metal anode and Cu cathode used to measure gas production.

Effects of NaCl Concentration on Gas Production Rates

To test the optimization of gas production rates by using different NaCl concentrations, 0, 10, 100, and 500 mM NaCl solutions with distilled H_2O was prepared. Then, 100 mL were distributed to vials and capped with a rubber stopper. Fe anodes were cut to measure 7.5 cm, and Cu cathodes were cut to be 5 cm in length. The filled vials and electrodes were autoclaved for sterility. Once sterile and cooled to room temperature, a Cu cathode and Fe anode was inserted into each vial through the rubber stopper. The assembled vials were connected to a power supply and set to 15 V for 10 minutes each. Each voltage was ran 3 times with 3 assembled vials to perform triplicates. Gas production was measured by inserting a syringe into the vial and observing the plunger displacement volume.

Antimicrobial Efficacy of Nanoparticles using 96 Well High Throughput

To test the antimicrobial efficacy of produced nanoparticles, 500 mM NaCl solution with distilled H_2O was prepared. Then, 100 mL were distributed to vials and capped with a rubber stopper. Fe and Zn anodes (7.5 cm), Cu cathodes (5 cm) were cut. The filled vials and electrodes

were autoclaved for sterility. Once sterile and cooled to room temperature, a Cu cathode and Fe anode was inserted into each vial through the rubber stopper. The assembled vials were connected to a power supply and set to 15 V for 10 minutes each. Afterward, 6 mL were extracted from each vial and collected in Eppendorf tubes. The collected solutions were centrifuged for 10 minutes, at $9 \times 1,000$ min^{-1}. The supernatant was removed, and the particulates were resuspended by adding TSA broth to the Eppendorf tubes.

Four 2 mL Eppendorf tubes were filled with 1.5 mL of TSA broth and inoculated with *E. coli* and *S. aureus* (2 tubes each). The optical density (OD_{600}) of each bacterial strain was measured using a Spectrophotometer before inoculated. The total volume of each well was 200 µL. The LB broth was distributed to the wells of both plates (one plate for Fe anode, one plate for Zn anode) in descending volumes down each column, with Row A having 200 µL and Row H having the least with 120 µL of broth (see Figure 4A). The resuspended nanoparticles were then distributed in ascending order to each well on its respective plate, with Row C having 5 µL and Row H having the most nanoparticles with 30 µL. Each bacteria strain was distributed at a constant volume of 50 µL to 3 adjacent columns from rows B to H. In both plates, Row A was used as a negative control and Row B was used as a positive control. After both the Fe and Zn anode plates are finished, the OD_{600} of the plates were taken at time zero using a plate reader. The plates were then incubated at 37 °C for 4 hours and then their OD_{600} were measured and recorded again.

Chemical Makeup and Nanostructure of Nanoparticles

When a voltage is applied to an Fe anode and Cu cathode to promote electrolysis of a saline solution, particulates are formed. These particulates have been identified as tribasic copper

chloride (TBCC). When a voltage is applied to a Zn anode and Cu cathode to promote electrolysis of a saline solution, particulates are formed on the Zn anode. These particulates fall from the anode and settle at the bottom of the vial, appearing as a white substance. To identify the particulates formed from the Zn anode, the vial was left untouched for 24 hours to allow the particulates to settle at the bottom. The rubber stopper was uncapped, and the supernatant saline solution was poured out, making sure not to pour out any of the particulates.

The remaining particulates were pipetted from the vial and onto an EZ Flow Membrane filter paper with the diameter of 47 mm and pore size of 0.45 µm, which was used as part of a vacuum device. The liquid was vacuumed through the filter paper and collected in a flask, leaving only the particulates to remain on top of the filter paper. The remaining particulates were then put in a vacuum chamber. All of the O_2 was removed from the vacuum chamber to continue to dry the nanoparticles. Once completely dried, the nanoparticles were weighed, placed in a tube and crushed into a fine powder. The powder was then sonicated, rinsed with distilled H_2O, centrifuged, then supernatant was discarded. The nanoparticles were resuspended with distilled H_2O and rinsed again. The washed nanoparticles were observed using a scanning electron microscope (SEM), and characterized using Energy Dispersive X-ray Spectroscopy (EDS) and X-Ray Diffraction (XRD).

WAVE Digester Design and MEC CH_4 Production

The CH_4 production of each MEC was measured using Gas Chromatography once a week for 8 weeks (Figure 1). Vertical WAVE digester is indicated by "V", and horizontal is indicated by "H". The sterile reactor was never inoculated with the mixed culture and acted as the negative control (see Table 1 for details of each category). As shown, there was no significant difference between voltage or WAVE digester design on CH_4 production concluding the 8-week study (Figure 2). Compared to the stationary, traditional anaerobic digester, none of the 700 mV applied MECs, despite WAVE digester design, had a significantly higher CH_4 accumulation after 8 weeks (p-value is 0.058). Compared to the stationary, traditional anaerobic digester, none of the 900 mV applied MECs, despite WAVE digester design, had a significantly higher CH_4 accumulation after 8 weeks (p-value is 0.568). Statistics were calculated using the Social Science Statistics' One-Way ANOVA Calculator.
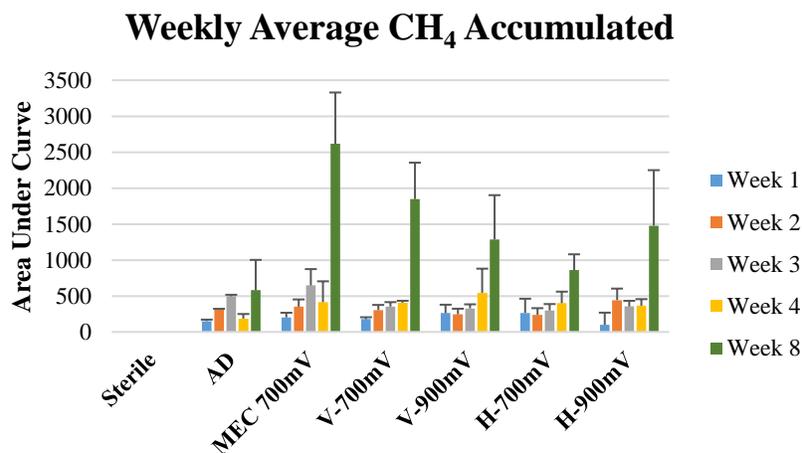

Figure 1. Weekly averages of CH_4 accumulation for each WAVE digester design.
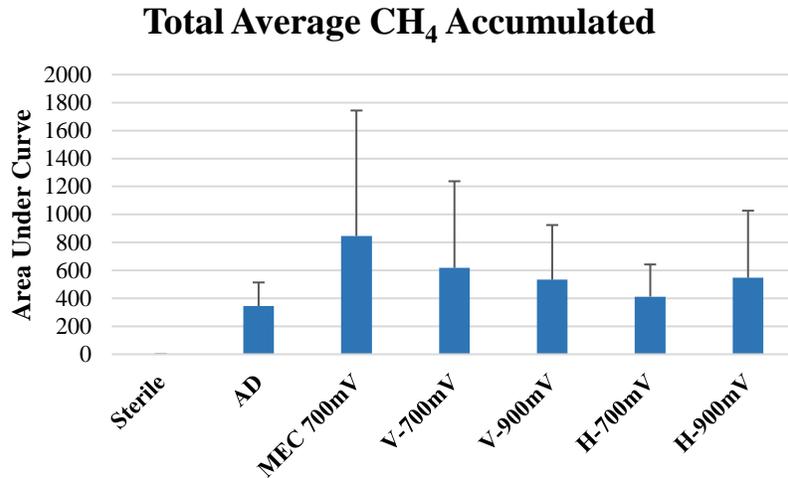
Total Average CH$_4$ Accumulated

Figure 2. Total average CH$_4$ accumulated for each WAVE digester design in the 8-week study.

Microbial Community Analysis

       After isolating the DNA from the mixed culture sample the total DNA concentration was measured using a NanoDrop Spectrophotometer, and the total DNA concentration was 54.9 ng/μL. Following isolation of DNA and DGGE analysis (Figure 3) of each digester category. The DNA sequencing was carried out using the Oxford Nanopore MinION DNA Sequencer. The results from the DNA sequencing were imported into the BLAST tool (NCBI). The most prevalent exo-electrogenic microorganisms of the mixed culture, which help produce CH$_4$, were *Geobacter sulfurreducens, Geobacter metallireducens, Geobacter pickeringii,* and *Geobacter anodireducens* (Figure 4). The phylogenetic tree of the identified microorganisms were also mapped out using the Geneious program (Figure 5).
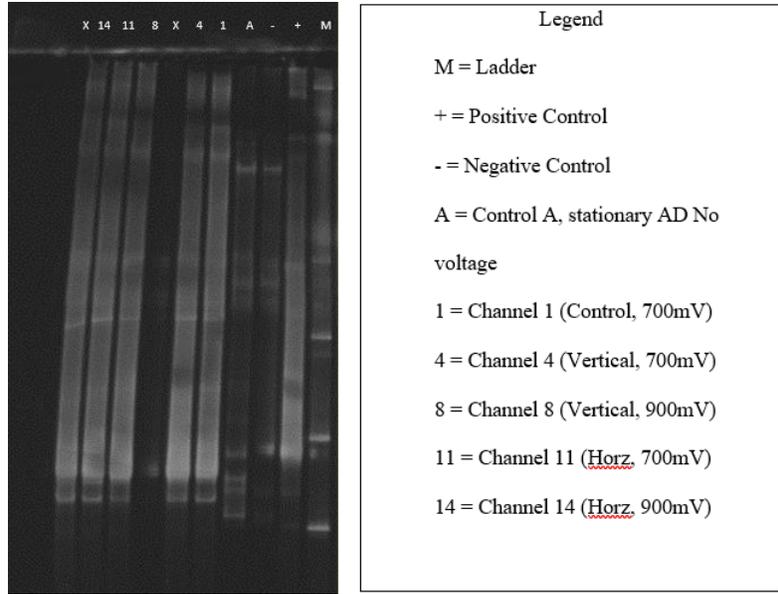
Figure 3. DGGE of DNA samples in reactors from each WAVE digester group.

Hit end ▼		Name	Description
3,328,582		CP010430	Geobacter sulfurreducens strain AM-1 genome
3,246,045		CP000148	Geobacter metallireducens GS-15, complete genome
2,912,166		CP009788	Geobacter pickeringii strain G13, complete genome
2,829,071		CP009788	Geobacter pickeringii strain G13, complete genome
2,780,416		CP010430	Geobacter sulfurreducens strain AM-1 genome
2,448,659		CP009788	Geobacter pickeringii strain G13, complete genome
2,421,300		CP014963	Geobacter anodireducens strain SD-1, complete genome
2,047,611		LT896716	Geobacter sp. DSM 9736 genome assembly, chromosome: I
1,920,361		LT896716	Geobacter sp. DSM 9736 genome assembly, chromosome: I
1,310,058		CP000148	Geobacter metallireducens GS-15, complete genome
1,224,160		AE017180	Geobacter sulfurreducens PCA, complete genome
1,208,758		AP017912	Geobacter sulfurreducens DNA, complete genome
1,195,042		CP002031	Geobacter sulfurreducens KN400, complete genome

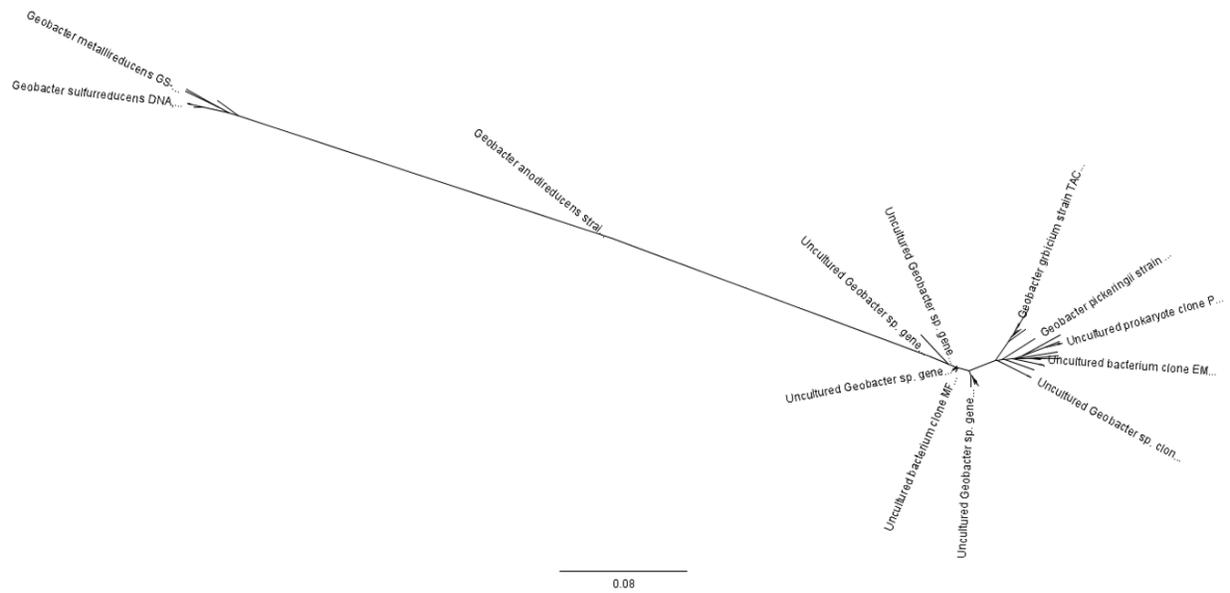Figure 4. Prevalent microbial species identified in the mixed culture of each MEC.

0.08

Figure 5. Phylogenetic linkage of identified microorganisms in the MECs.

Inhibition of Waterborne Virus and Bacteria

After performing triplicate plaque assay analyses of the effect of an Fe anode and Cu cathode at 0 V, 10 V, and 15 V, the results were graphed and compared (Figure 6). As shown, the greatest viral activity was at 0 V, and the least at 15 V being 5 magnitudes of order less than at 0 V. The P-value between 0 V and 10 V is 0.0214, P-value between 0 V and 15 V is 0.0212, and the P-value between 10 V and 15 V is 0.0038. Statistics were done using GraphPad's t-test calculator.
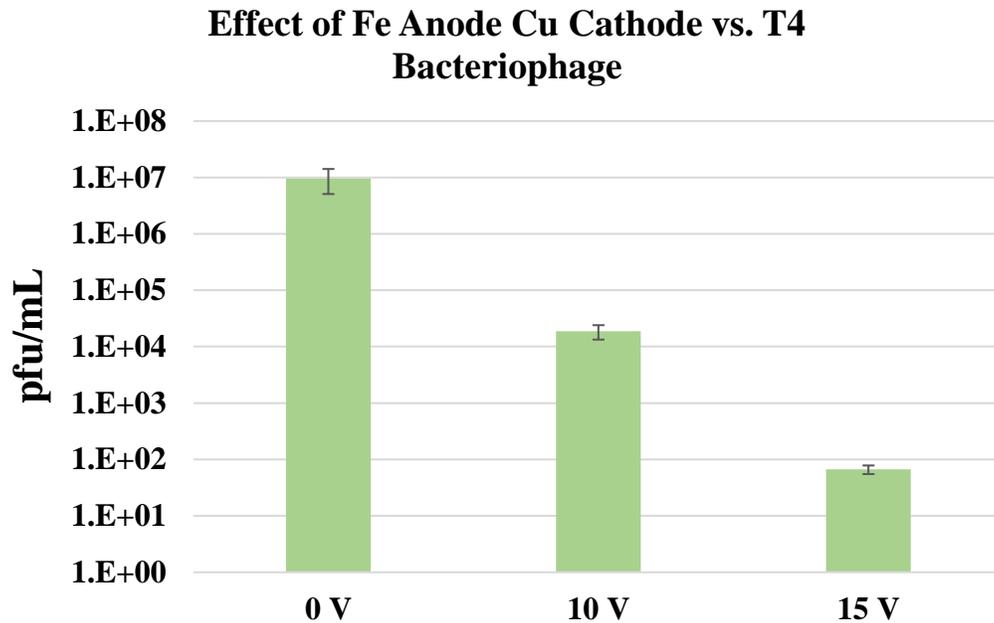
**Effect of Fe Anode Cu Cathode vs. T4
Bacteriophage**

Figure 6. Inhibitory effect of electrode metals (Fe and Cu) on waterborne virus T4 Bacteriophage at 0 V, 10 V, and 15 V.

Effect of Metals on Gas Production

At 5 V and 10 V, Al and Zn both produced more gas than Fe (see Figure 7). Although, Zn and Al had no significant difference between each other with a P-value of 0.2116 at 5 V, and a P-value of 0.4885 at 10 V. However, when 15 V was applied, Al produced significantly more gas than Fe, Zn, and Ti (P < 0.05). Statistics were done using GraphPad's t-test calculator.
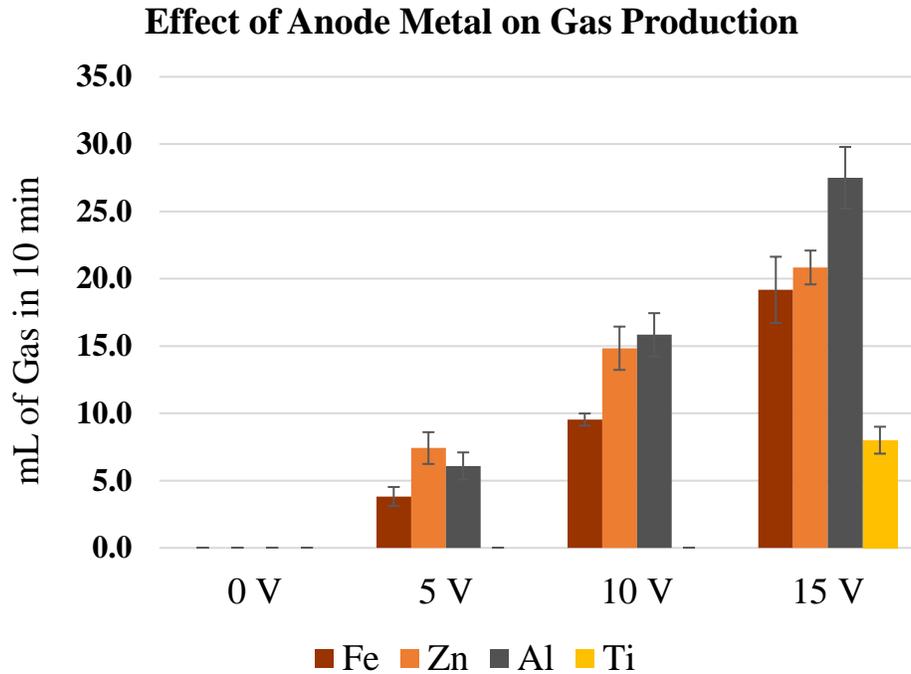
Effect of Anode Metal on Gas Production

Figure 7. Showing the effect of anode metal on gas production.

Effects of NaCl Concentrations on Gas Production Rates

The gas production increased as the NaCl concentration increased (Figure 8). The highest gas production, 41.5 mL, was seen with 500 mM. Whereas at 100 mM, 10 mM, and 0 mM, the gas production was 20.6 mL, 4.5 mL, and 0 mL, respectively. Each concentration's gas production was significantly different with the P-value < 0.0001 between all groups. Statistics were done using GraphPad's t-test calculator.
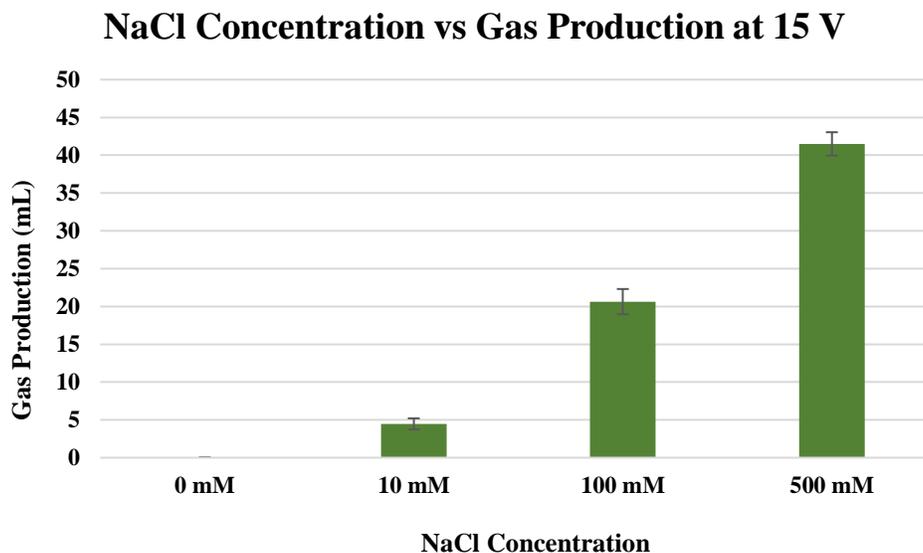
NaCl Concentration vs Gas Production at 15 V

Figure 8. Influence of electrolyte NaCl concentration on gas production at 15 V.

Antibacterial Efficacy of Nanoparticles

Following 4 hours of incubation at 37.0 °C, the antimicrobial effect of one Fe anode and one Zn anode were measured (see Figure 9 and Figure 10, respectively). The P-values between *E. coli* and *S. aureus* after 4 hours of incubation at all nanoparticle concentrations 5 – 30 mg/µL, regardless of metal used, exceeded the 0.05 significance level. Following 24 hours of incubation, the antimicrobial effect of one Fe anode and one Zn anode were also measured (see Figure 11 and Figure 12, respectively). After 24 hours, only Zn nanoparticles showed a significant difference between *E. coli* and *S. aureus*. At Zn concentrations of 15 mg/µL, 20 mg/µL, 25 mg/µL, and 30 mg/µL the P-values were 0.0017, 0.0039, 0.0004, and < 0.0001, respectively. It is hypothesized the initial inoculum was lysed at high concentration of nanoparticles and caused the optical density to fall below zero. Statistics were done using GraphPad's t-test calculator.

Fe Anode 4 Hours

Figure 9. Effect of Fe anode derived nanoparticles on gram negative, *E. coli*, and gram positive,

S. aureus, microorganisms' growth following 4 hours of incubation.

Zn Anode 4 Hours

Figure 10. Effect of Zn anode derived nanoparticles on gram negative, *E. coli*, and gram positive,

S. aureus, microorganisms' growth following 4 hours of incubation.
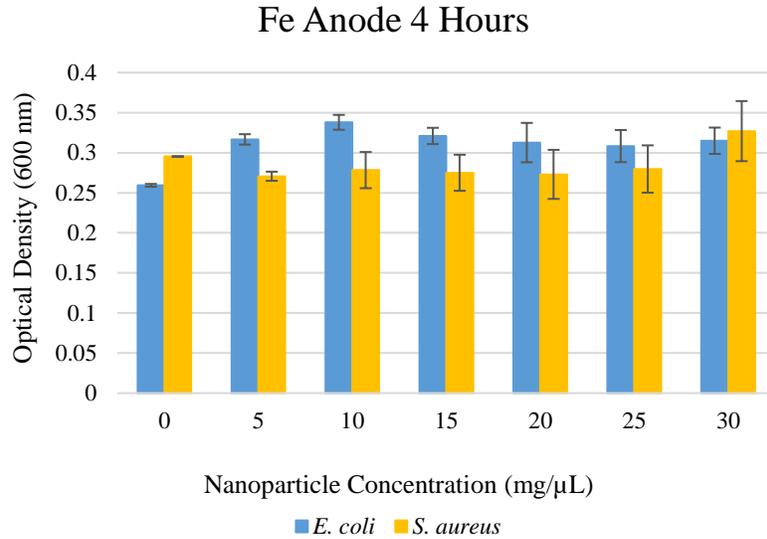
Fe Anode 24 Hours

Figure 11. Effect of Fe anode derived nanoparticles on gram negative, *E. coli*, and gram positive, *S. aureus*, microorganisms' growth following 24 hours of incubation.
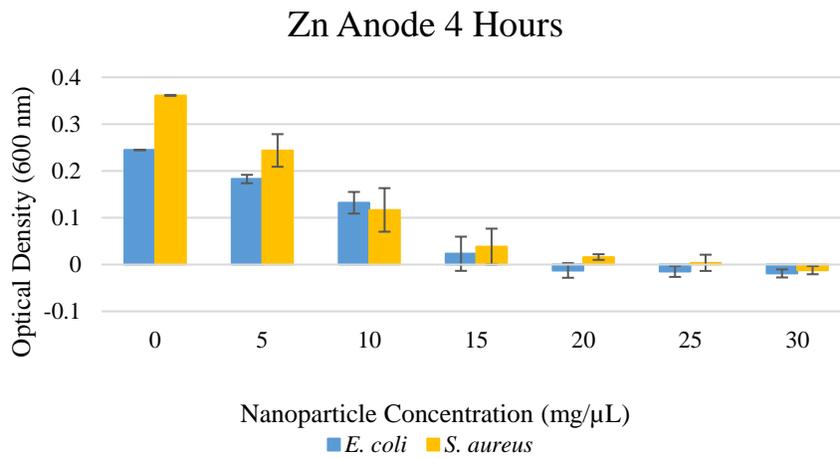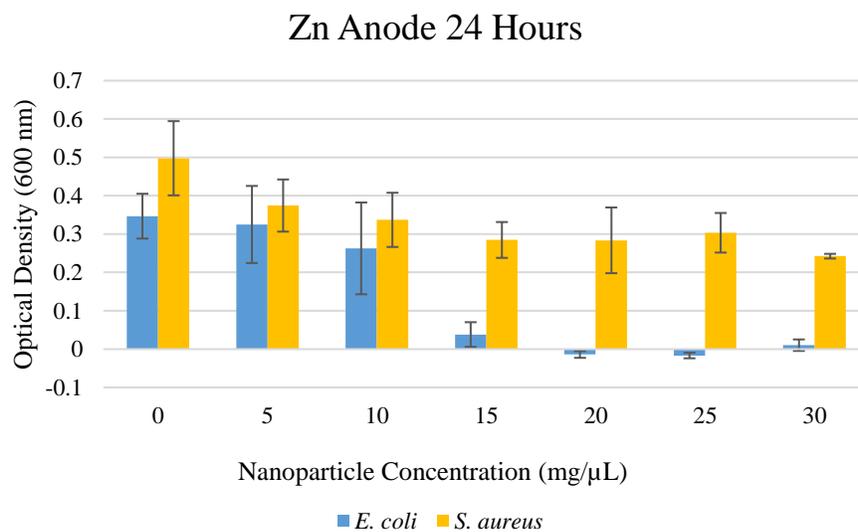
Zn Anode 24 Hours

Figure 12. Effect of Zn anode derived nanoparticles on gram negative, *E. coli*, and gram positive, *S. aureus*, microorganisms' growth following 24 hours of incubation.
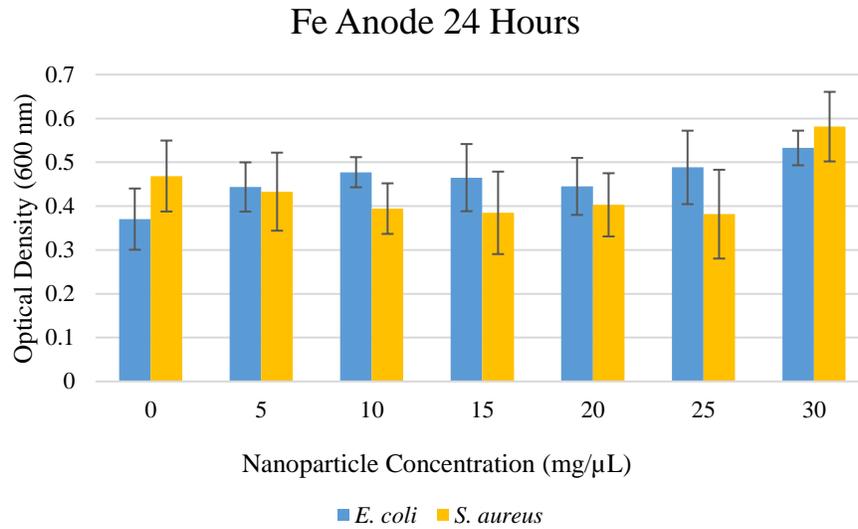
Chemical Makeup and Nanostructure of Nanoparticles

By using Scanning Electron Microscope (SEM), the nanostructure and size of the Zn nanoparticles were able to be observed (Figure 13). The chemical makeup of the nanoparticles was determined using Energy-dispersive X-ray spectroscopy (EDS) (see Figure 14 and Table 1). The nanoparticles were identified as ZnO by using XRD (Figure 15). After identifying the nanoparticles as ZnO, it was confirmed using IR spectroscopy (Figure 16).
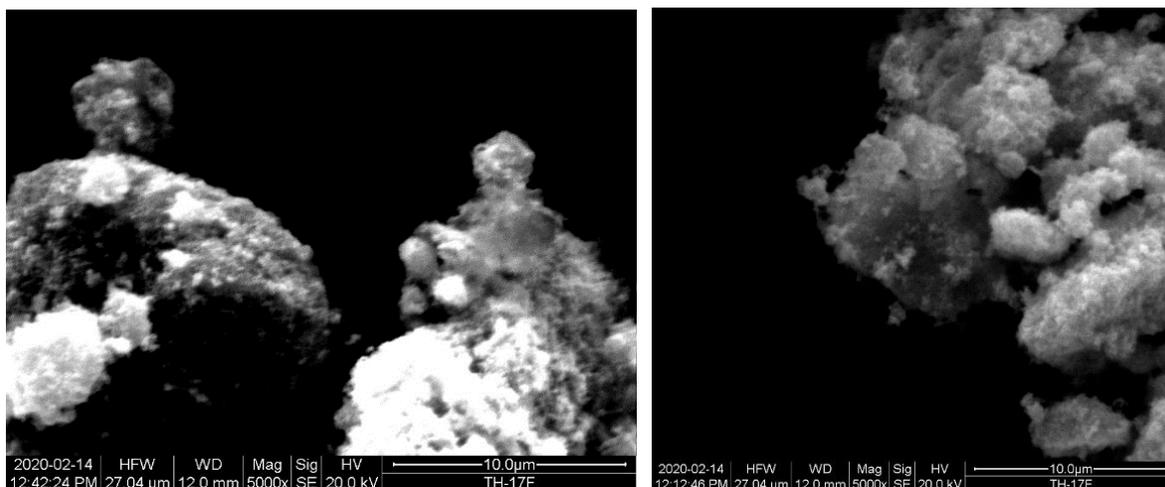
Figure 13. SEM images of washed Zn nanoparticles.
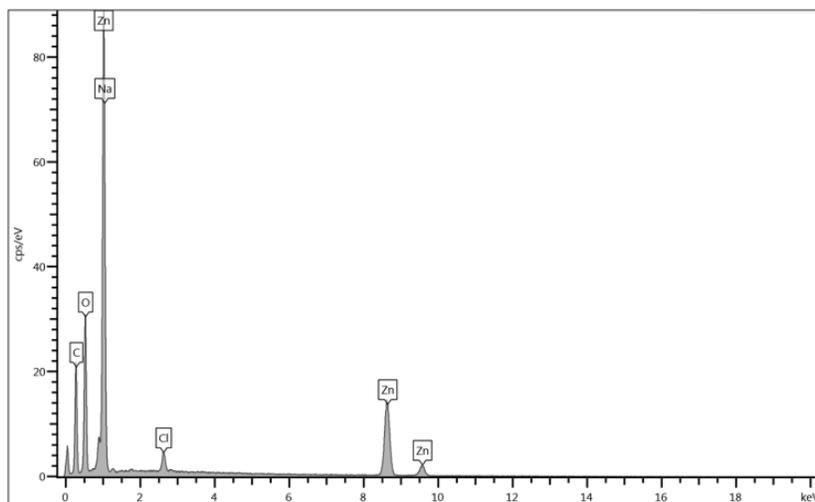
Figure 14. Energy-dispersive X-ray spectroscopy reveals detected elements of a washed Zn nanoparticle using EDS.

Result Type	Weight %			
Statistics	O	Na	Cl	Zn
Max	30.25	14.08	2.04	66.56
Min	22.29	10.11	1.00	56.66
Average	27.04	12.26	1.22	59.48
Standard Deviation	2.90	1.66	0.46	4.06

Table 1. Percentage by weight of each element detected in washed Zn nanoparticles using EDS.

Figure 15. XRD analysis of washed ZnO nanocomposite.

Figure 16. Showing results of washed ZnO nanoparticles after IR detection.

Discussion

By 1 week of 25°C incubation, detectable methane was produced in both stationary and moving reactors, indicating early growth of methanogens (Figure 1). No significant early difference in biogas production was observed in vertical vs horizontally mixed digesters. There was no statistical difference in the average methane production observed in different WAVE digester configurations by the 8-w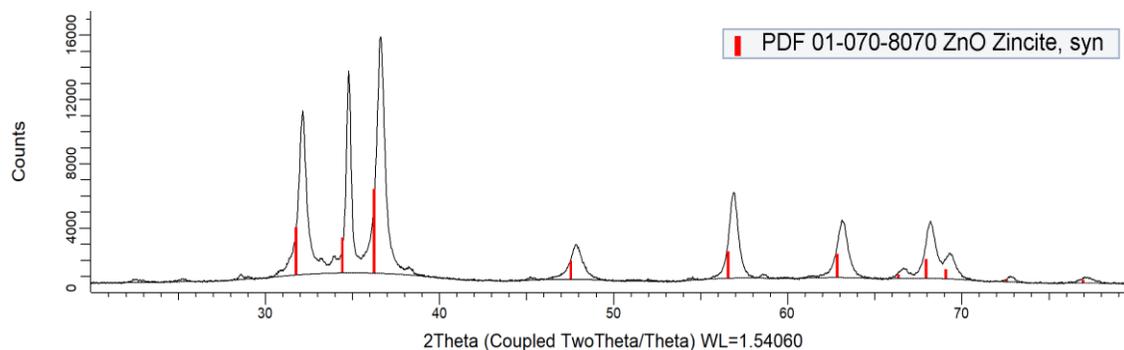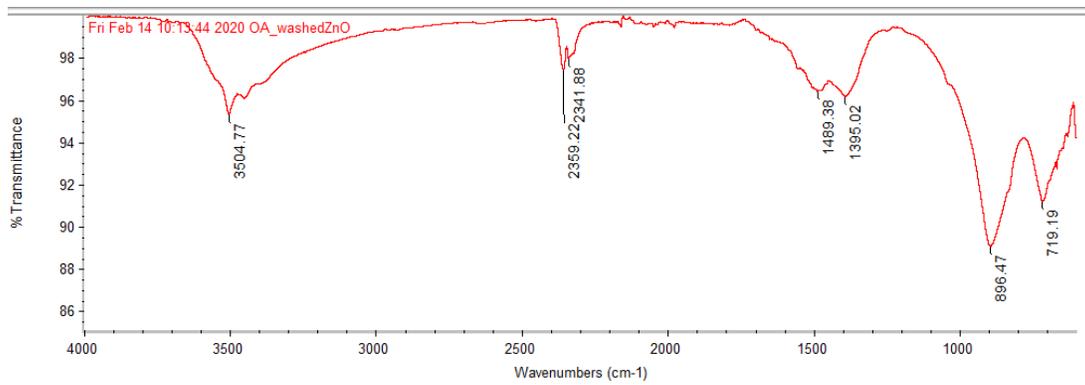eek time point. These results suggest the current WAVE digester design may not provide for enhanced CH_4 production compared to unmixed bioelectrochemically active anaerobic digesters, as initially hypothesized.

Electrogenic microbial communities, including biofilm associated species, developed during the 8-week study within CH_4 producing reactors as revealed by metagenomic methods (Figure 3). Prevalent within methanogenic reactors were species of the know electrogenic bacterial genus *Geobacter* (Figure 4). A biofilm is an assemblage of microbial cells that are not easily removed by gentle rinsing from a surface and enclosed in a matrix of primarily polysaccharide material (Donlan, 2002). Microbial biofilms also allow microbial cells to communicate easily with each other and provides a setting for bacteria to communicate using chemical signals (*Microbes in a Biofilm*). When these chemical signals are sensed by cells in the biofilm, communication between neighboring cells can cause the microbes to behave differently (*Microbes in a Biofilm*). Because the microorganisms were constantly disturbed due to the motion of each WAVE digester, the microbial biofilm did not sufficiently form on the electrodes of the reactors. Also, perhaps breaking down organic matter in the wastewater before inoculating the reactors would be better for optimal CH_4 production. Possible improvements might be to

provide for an available larger surface area of the substrate and inoculating the reactors while stationary could efficiently produce CH_4 and allow the biofilm to form.

The most prevalent microorganisms of the mixed culture, which help produce CH_4, were of the *Geobacter* genus (Figure 4). *Geobacter* are types of exoelectogenic bacteria that produce higher current densities than any other known organism in microbial fuel cells (Lovley et al., 2011). They also are very useful in microbial electrolysis cells as well (Rousseau et al., 2020). Electrotrophic microorganisms on the MEC cathode accept electrons to store input electrical energy as chemical fuel bonds in CH_4. *Geobacter* species are common colonizers of the anode in MECs and harvest electricity from organic wastes to donate electrons to electrotrophic microorganisms (Lovley et al., 2011). When the DGGE was completed, the "Control A" reactor, which was stationary and no applied voltage, was not as concentrated with bacteria (i.e. fewer bands) than the reactors with a constant current (Figure 3). The control reactors also produced less CH_4 than reactors that were constantly mixed with the vertical and horizontal WAVE digesters (Figures 1, 2).

Removal of organic chemicals is but one aspect of wastewater treatment. Equally, if not more important from a Public Health standpoint is the removal or inactivation or pathogenic microorganisms including various viruses and bacteria (Ramírez-Castillo et al., 2015). To date, research into the antimicrobial efficacy of energy storing bioelectrochemical and electrochemical systems is limited. In the current study, triplicate plaque assay analyses were performed to investigate the effect of an Fe anode and Cu cathode at 0 V, 10 V, and 15 V. The results showed that 15 V has the greatest effect on T4 Bacteriophage inhibition (Figure 6). The formation of TBCC is likely effective in inhibiting viral activity (Espinosa et al., 2017) but and is most efficacious when used in conjunction with an elevated applied electrical current of 15 V. To

sufficiently reduce waterborne viruses from water, a voltage of 15 V can be applied to the water to kill a waterborne virus like T4 Bacteriophage.

When testing the effect of metals on gas production Ti did not have any gas production until 15 V were applied (Figure 7). Titanium is resistant to corrosion due to its low reactivity and high oxidation states. It has a high affinity for oxygen and forms a tight titanium oxide when exposed to air or most other fluids containing oxygen (Zhang et al., 2020). In contrast, Al, Zn, and Fe reacted at all applied voltages (Figure 7). The results of each metal's effect on gas production was expected. The more highly reactive, readily oxidized metals such as Al and Zn metals providing more electrons for copious gas formation. Headspace gas formed revealed H_2, as indicated by Gas Chromatography analysis (Figure 5A).
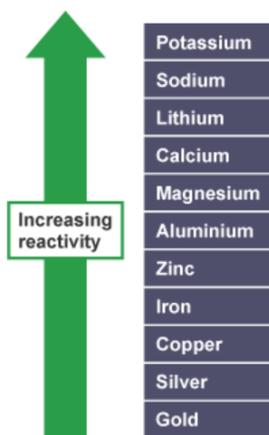
Figure 17. Common metals and their reactivity levels.

Voltage is a determining factor in antimicrobial effectiveness of these metallic nanoparticle-forming electrochemical systems, and 15 V had greatest antiviral activity. Although aluminum outperformed all metals at 15 V, Zn and Al are very similar in terms of overall gas production. The highest salt concentration tested, 500 mM, provided the most gas production

(Figure 8). Use of a Zn anode demonstrated greater antimicrobial effects on both bacteria strains tested, rather than Fe (Figures 9, 10, 11, 12). The nanoparticles produced after applying electrical current to a Zn anode and Cu cathode were identified as ZnO (Figures 14, 15, 16). The elements Na and Cl were detected using EDS likely due to the solution containing 500 mM NaCl (Table 1). Although the Zn nanoparticles were washed before experimentation of the chemical makeup, detectable traces of NaCl still remained.

There are several practical applications for the use of ZnO. Products such as sunscreen, ointments, lotion, and even food products like cereal have ZnO in them. Zn is a very important trace element in all living systems from animals to humans, and it plays an essential role in many metabolic processes of the body such as cell division, by regulating the synthesis of protein and DNA (Geetha et al., 2020). ZnO is also a predominant source of Zn used by the animal feed industry, and is the most commonly used Zn supplement with high antibacterial activity, antifungal, and growth promoter ability (Mohd Yusof et al., 2019). ZnO generates H_2O_2 which can pass through cell walls, disrupt metabolic processes, and inhibit the microbial growth (Geetha et al., 2020). The affinity of ZnO toward the bacterial cell is the most important factor for antibacterial activity (Yazdankhah et al., 2014). ZnO is regarded as generally recognized as safe and effective (GRASE) by the Food and Drug Administration (Commissioner, 2020).

In summary, WAVE digesters worked to generate CH_4 but still suffered from slow such a startup (approximately 30 days). Therefore, we sought a faster, more efficient means of storing renewable energy that also provided for additional benefits such as H_2O disinfection and nanoparticle formation. Antimicrobial ZnO nanoparticle formation was proven and is recommended because it is a common, low cost and widely available, scrap metal.

Future studies should investigate combinations of different metals and voltages to test gas production. Also, look at different microorganisms such as parasite cysts, *Pseudomonas fluorescens*, or *Bacillus subtilis* to test waterborne virus inhibition. Results from this study can help future experimental designs regarding anaerobic digestion, gas production, and waterborne virus inhibition as well.

References

Alcántara-Hernández, R. J., Taş, N., Carlos-Pinedo, S., Durán-Moreno, A., & Falcón, L. I. (2017). Microbial dynamics in anaerobic digestion reactors for treating organic urban residues during the start-up process. *Letters in Applied Microbiology*, *64*(6), 438–445. https://doi.org/10.1111/lam.12734

Bajracharya, S., Sharma, M., Mohanakrishna, G., Dominguez Benneton, X., Strik, D. P. B. T. B., Sarma, P. M., & Pant, D. (2016). An overview on emerging bioelectrochemical systems (BESs): Technology for sustainable electricity, waste remediation, resource recovery, chemical production and beyond. *Renewable Energy*, *98*, 153–170. https://doi.org/10.1016/j.renene.2016.03.002

Choi, K.-S., Kondaveeti, S., & Min, B. (2017). Bioelectrochemical methane (CH4) production in anaerobic digestion at different supplemental voltages. *Bioresource Technology*, *245*, 826–832. https://doi.org/10.1016/j.biortech.2017.09.057

Commissioner, O. of the. (2020, February 20). *FDA advances new proposed regulation to make sure that sunscreens are safe and effective*. FDA; FDA. http://www.fda.gov/news-events/press-announcements/fda-advances-new-proposed-regulation-make-sure-sunscreens-are-safe-and-effective

Donlan, R. M. (2002). Biofilms: Microbial Life on Surfaces. *Emerging Infectious Diseases*, *8*(9), 881–890. https://doi.org/10.3201/eid0809.020063

Eerten-Jansen, M. C. A. A. V., Heijne, A. T., Buisman, C. J. N., & Hamelers, H. V. M. (2012). Microbial electrolysis cells for production of methane from CO2: Long-term performance and perspectives. *International Journal of Energy Research*, *36*(6), 809–819. https://doi.org/10.1002/er.1954

Espinosa, C. D., Fry, R. S., Usry, J. L., & Stein, H. H. (2017). Copper hydroxychloride improves growth performance and reduces diarrhea frequency of weanling pigs fed a corn-soybean meal diet but does not change apparent total tract digestibility of energy and acid hydrolyzed ether extract. *Journal of Animal Science*, *95*(12), 5447–5454. https://doi.org/10.2527/jas2017.1702

Facts About Anaerobic Digesters: What are the Pros & Cons? (2018, September 20). Green Coast. https://greencoast.org/facts-about-anaerobic-digesters/

Geetha, K., Chellapandian, M., Arulnathan, N., & Ramanathan, A. (2020). Nano zinc oxide—An alternate zinc supplement for livestock. *Veterinary World*, *13*(1), 121–126. https://doi.org/10.14202/vetworld.2020.121-126

Holm-Nielsen, J. B., Al Seadi, T., & Oleskowicz-Popiel, P. (2009). The future of anaerobic digestion and biogas utilization. *Bioresource Technology*, *100*(22), 5478–5484. https://doi.org/10.1016/j.biortech.2008.12.046

Lovley, D. R., Ueki, T., Zhang, T., Malvankar, N. S., Shrestha, P. M., Flanagan, K. A., Aklujkar, M., Butler, J. E., Giloteaux, L., Rotaru, A.-E., Holmes, D. E., Franks, A. E., Orellana, R., Risso, C., & Nevin, K. P. (2011). Geobacter: The microbe electric's physiology, ecology, and practical applications. *Advances in Microbial Physiology*, *59*, 1–100. https://doi.org/10.1016/B978-0-12-387661-4.00004-5

Microbes in a Biofilm Can Communicate With Each Other. (n.d.). Retrieved March 12, 2020, from https://www.cs.montana.edu/webworks/projects/stevesbook/contents/chapters/chapter001/section006/green/page003.html

Mohd Yusof, H., Mohamad, R., Zaidan, U. H., & Abdul Rahman, N. A. (2019). Microbial synthesis of zinc oxide nanoparticles and their potential application as an antimicrobial

agent and a feed supplement in animal industry: A review. *Journal of Animal Science and Biotechnology*, *10*, 57. https://doi.org/10.1186/s40104-019-0368-z

Quinn, M. (2019, March 18). What is Wastewater: Where Does it Come from and Where Does it Go? *ASL Limited*. https://www.asllimited.co.uk/blog/what-is-wastewater-where-does-it-come-from-and-where-does-it-go/

Ramírez-Castillo, F. Y., Loera-Muro, A., Jacques, M., Garneau, P., Avelar-González, F. J., Harel, J., & Guerrero-Barrera, A. L. (2015). Waterborne Pathogens: Detection Methods and Challenges. *Pathogens*, *4*(2), 307–334. https://doi.org/10.3390/pathogens4020307

Rousseau, R., Etcheverry, L., Roubaud, E., Basséguy, R., Délia, M.-L., & Bergel, A. (2020). Microbial electrolysis cell (MEC): Strengths, weaknesses and research needs from electrochemical engineering standpoint. *Applied Energy*, *257*, 113938. https://doi.org/10.1016/j.apenergy.2019.113938

U.S. energy facts—Data and statistics—U.S. Energy Information Administration (EIA). (n.d.). Retrieved February 27, 2020, from https://www.eia.gov/energyexplained/us-energy-facts/data-and-statistics.php

US EPA, O. (2016, April 15). *Basic Information about Landfill Gas* [Overviews and Factsheets]. US EPA. https://www.epa.gov/lmop/basic-information-about-landfill-gas

Wall, J., Harwood, C. S., & Demain, A. L. (2008). *Bioenergy*. ASM Press. http://ebookcentral.proquest.com/lib/wcupa/detail.action?docID=476459

Xu, S., Zhang, Y., Luo, L., & Liu, H. (2019). Startup performance of microbial electrolysis cell assisted anaerobic digester (MEC-AD) with pre-acclimated activated carbon. *Bioresource Technology Reports*, *5*, 91–98. https://doi.org/10.1016/j.biteb.2018.12.007

Yazdankhah, S., Rudi, K., & Bernhoft, A. (2014). Zinc and copper in animal feed—Development of resistance and co-resistance to antimicrobial agents in bacteria of animal origin. *Microbial Ecology in Health and Disease*, *25*. https://doi.org/10.3402/mehd.v25.25862

Zhang, X., Wan, Y., Ren, B., Wang, H., Yu, M., Liu, A., & Liu, Z. (2020). Preparation of Superhydrophobic Surface on Titanium Alloy via Micro-milling, Anodic Oxidation and Fluorination. *Micromachines*, *11*(3). https://doi.org/10.3390/mi11030316

Zhao, Z., Li, Y., Quan, X., & Zhang, Y. (2017). Towards engineering application: Potential mechanism for enhancing anaerobic digestion of complex organic waste with different types of conductive materials. *Water Research*, *115*, 266–277. https://doi.org/10.1016/j.watres.2017.02.067

Zhao, Z., Zhang, Y., Yu, Q., Dang, Y., Li, Y., & Quan, X. (2016). Communities stimulated with ethanol to perform direct interspecies electron transfer for syntrophic metabolism of propionate and butyrate. *Water Research*, *102*, 475–484. https://doi.org/10.1016/j.watres.2016.07.005
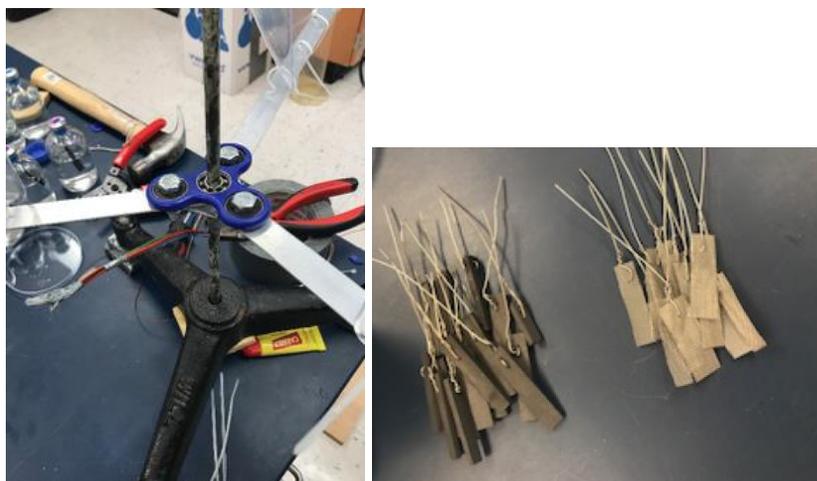
Appendix

Figure 1A. Some of the materials needed for the WAVE digesters. Depicted on the left is the foundation of the vertical WAVE digester. The anodes were made of graphite and the cathodes were made of steel mesh.

Figure 2A. The vertical WAVE digester is to the far left, and the horizontal WAVE digester is in the middle. The wires were soldered from the potentiostat onto the anode and cathode of each reactor so the proper voltage for each respective reactor could be applied.

Reactor #	Channel		Voltage
4	1	Controls	700mV
2	2		
7	3		
12	4	Vertical Rotor	700mV
11	5		
10	6		
Mixed Culture	7		
3	8	Vertical Rotor	900mV
5	9		
6	10		
15	11	Horizontal Rotor	700mV
14	12		
13	13		
1	14		900mV
8	15		
9	16		

Figure 3A. The reactor number was recorded to keep track of each reactor in the experiment.

Each reactor was assigned a channel from the potentiostat and set at either 700 mV or 900 mV.

The reactors were also put into groups of 3 for each respective category tested in the experiment.

96 Well Plate Rows	Nanoparticle Concentration (mg/μL)	Broth Volume (μL)	Bacteria Volume (μL)
A	0	200	0
B	0	150	50
C	5	145	50
D	10	140	50
E	15	135	50
F	20	130	50
G	25	125	50
H	30	120	50

Figure 4A. The nanoparticle concentration increased from Row B to Row H. Row A was used as a negative control, with no bacteria or nanoparticles in the wells of Row A. Each well had a total volume of 200 μL.

Component	Retention	Area	External	Units	Area %	Norm area %
H2 TCD	1.786	0.0974	0.0055	uL	0.2694	0.0140
O2	2.496	7.1500	7.2357	uL	19.77...	18.3279
N2	2.800	26.7328	32.1631	uL	73.94...	81.4685
uk	3.656	0.1946	0.0748		0.5383	0.1895
CH4 TCD	0.000	0.0000	0.0000	uL	0.0000	0.0000
CO TCD	0.000	0.0000	0.0000		0.0000	0.0000
CO2 TCD	0.000	0.0000	0.0000	uL	0.0000	0.0000
		34.1748	39.4791		100.0...	100.0000

Figure 5A. Gas Chromatography analysis confirming the formation of H_2 produced from electrolysis using Fe, Al, Zn, and Ti anodes with a Cu cathode.